Solar Assisted Heat Pump Systems Based on Hybrid PVT Collectors for the Provision of Hot Water, Cooling and Electricity in Buildings

María Herrando[1], Adriana Coca-Ortegón[2], Isabel Guedea[2] and Norberto Fueyo

[1] Fluid Mechanics Group, School of Engineering and Architecture University of Zaragoza, Zaragoza (Spain)

[2] EndeF Engineering S.L., Zaragoza (Spain)

Abstract

This work aims to assess the techno-economic performance of solar hybrid PVT collectors integrated via thermal storage tanks with an air-to-water reversible vapour-compression (rev-VC) unit. Real weather data along with the actual heating, cooling and electricity demands of an industrial building are inputs to the transient model. Different configurations are analysed varying the number of PVT collectors and the storage tanks' volumes. Radiative cooling of the PVT collectors is also considered to satisfy the cooling demand. The results show that the proposed systems have the potential to cover 19.2% to 46.5% of the cooling demand through radiative cooling, depending on the number of PVT collectors, thus decreasing the electricity consumed by the rev-VC. All the analysed configurations can also cover >60% of the demand for heat at 60ºC and between 31.7% to 48.5% of the electricity demand of the analysed building. The systems have a payback time of <10 years. The selected system, consisting of 16 PVT collectors (26.1 m^2) and 2 tanks of 350 L each one, is currently being manufactured and will be tested under real weather conditions from middle September 2020.

Keywords: hybrid PVT collector, energy modelling, heat pump, payback time, radiative cooling

1. Introduction

Heating and cooling (H/C) is the largest energy-consuming application in Europe, responsible for 51% of the total final energy demand (580 Mtoe) (European Union, 2018). Most of the demand is for space heating (52%) process heating (30%) and water heating (10%), with space cooling demand being still limited but fast-growing. Buildings are the main consumers of H/C: 45% of the energy for H/C is used in the residential sector, 37% in industry and 18% in services (European Commission, 2016). However, the share of renewable energy (RES) for H/C in 2016 was only 19.1% (European Union, 2018). Thus, the development and implementation of RES for building H/C are essential for displacing fossil-fuel utilisation, reducing emissions and increasing the share of RES. Solar heating and cooling (SHC) technologies appear as an attractive decarbonisation alternative, as they can provide both heating and cooling.

In recent years, hybrid photovoltaic-thermal (PVT) collectors are gaining increasing attention both in research and in applications, as they combine the output of photovoltaic (PV) and solar thermal systems from the same aperture area: they generate both electricity and useful heat simultaneously (Herrando et al., 2019b), with higher overall efficiency than the separate systems (Das et al., 2018; Joshi and Dhoble, 2018). Further, the integration of PVT collectors with H/C technologies allows the simultaneous generation of hot water, cooling and electricity, and thus has the potential to cover a significant fraction of the energy demands of buildings (Herrando et al., 2019a). The relevance and potential of PVT collectors and their integration with other components to obtain new solutions in HVAC systems are confirmed with the creation of Task 60 of PVT systems of the SHC programme of the IEA (IEA, 2018). However, most of the research in the literature focuses on SHC technologies that use solar thermal collectors (Ge et al., 2018) for solar cooling (Leonzio, 2017; Montagnino, 2017), or PV panels integrated into solar assisted heat pump (SAHP) systems for solar heating (Bellos et al., 2016; Thygesen and Karlsson, 2014; Vaishak and Bhale, 2019).

This research proposes solar combined cooling, heating and power (S-CCHP) systems based on PVT collectors to help decarbonising industrial buildings. The aim here is to analyse the techno-economic performance of several S-CCHP system configurations and select the system size to build a pilot plant that will provide cooling, heating and power to an industrial building. To this end, a transient model is developed that features PVT collectors,

doi:10.18086/eurosun.2020.05.10 Available at http://proceedings.ises.org

thermal storage and an air-to-water (a-w) reversible vapour-compression (rev-VC) unit (also known as solar-assisted heat pump, SAHP).

2. Methodology

The proposed S-CCHP systems are modelled in dynamic simulation software, TRNSYS (Klein, 2016), where the real heating, cooling and electricity demands of an industrial building located in Zaragoza (Spain) are used as inputs to the model to undertake transient simulations with a 15-min time-step for a period of one year. The existing scenario of energy demand and supply is considered to estimate the annual cost savings with the proposed systems, considering current utility prices. The systems' payback time is also estimated.

2.1. Energy demand of the industrial building

The industrial building consists of two main areas: the manufacturing area and the office area. The manufacturing area includes lighting and different electrically powered devices and equipment. This area also demands hot water at 60 ºC for the shower section. The office area has a demand for heating and cooling, which are currently satisfied by an air-to-air reversible vapour compression unit, powered by electricity. This area also includes lighting and other small electrical devices (e.g. computers, printers, etc.).

Table 1 presents the real energy demand of the industrial building, including heat at 60ºC, space heating or low-temperature heat (30-35ºC), cooling (18-23ºC) and electricity consumption (for lighting and other electrical devices). The total annual electricity consumption in the industrial building is 24,566 kWh, of which 11,728 kWh (48%) corresponds to the thermal energy demand. Specifically, the largest thermal energy demand is cooling, accounting for 39%, followed by low-temperature heat and heat at 60 ºC demands (35% and 26% respectively).

Tab. 1: Annual energy demands and their corresponding energy consumptions for the industrial building under study.

Description	**Heat at 60ºC ($Q_{H60,dem}$)**	**Low-temperature heat ($Q_{lth,dem}$)**	**Cooling ($Q_{Cool,dem}$)**	**Electricity ($E_{El,dem}$)**
Schedule	Mon - Fri (8-18h)	Mon - Fri (8-18h)	Mon - Fri (8-18h)	Baseload (24 h/day) + Higher consumption Mon - Fri (8-18h)
Temperature (ºC)	60	30-35	7 a 12	
Annual demand (kWh/year)	2,998	9,772	9,193	12,548
Existing system	Electrical heater	Air-to-air heat pump		-
Current system efficiency	0.98	2.36	2.03	-
Annual consumption (kWh/year)	3,060	4,140	4,528	12,548

2.2 Solar Combined Cooling Heating and Power System

The S-CCHP system consists of PVT collectors, an a-w rev-VC unit and two parallel storage tanks, the hot-water tank to satisfy heat at 60 °C and the inertia tank to satisfy low-temperature heating or cooling demands. Depending on the tanks' temperature and the PVT collectors' temperature, the thermal output of the PVT collectors is directed to one of the two tanks through an active closed-loop system with a bypass valve controlled by a differential temperature controller (Figure 1). When there is cooling demand, water circulates through the PVT collectors at night to cool the water in the inertia tank (radiative cooling). In both heating and cooling modes, the a-w rev-VC unit acts as an auxiliary heater/cooler, to reach the set-point temperatures of the building's thermal demand. The rev-VC unit is electrically powered by the PVT collectors, and the PVT electrical output not consumed by the rev-VC unit is used to match the industry's electricity demand. The main system components (PVT collectors, storage tanks, rev-VC unit) are implemented in the model modifying the corresponding types to match the real characteristics and performance of the commercial units.

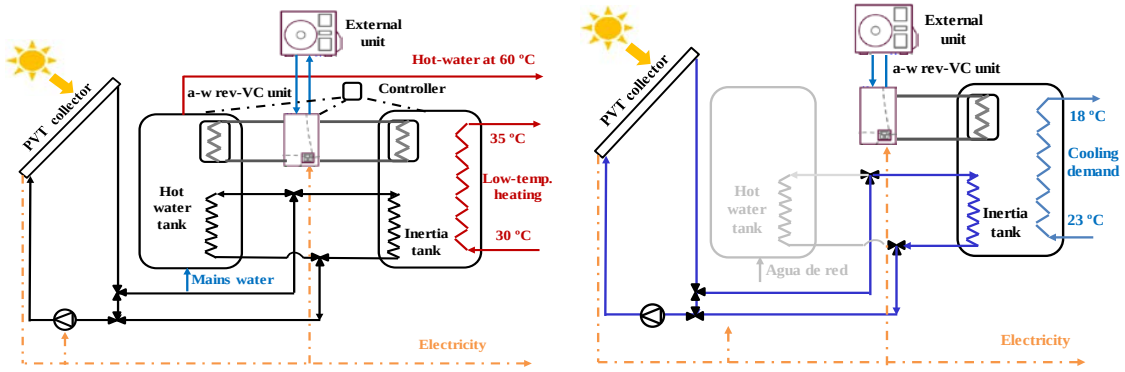

Fig. 1: Schematic diagrams of the S-CCHP systems in (left) heating mode and (right) cooling mode.

PVT collector

The ECOVOLT collector (uncovered, 300 W_p, 1.63 m^2 aperture area) is used in this work (EndeF, 2017). Type 50d is modified and adjusted to match the thermal efficiency (η_{th}) and the electrical efficiency (η_e) curves provided by the manufacturer (see Eqs. (1-3)). PVT collectors are connected in parallel so as flow-rate, inlet and outlet water temperatures all the same in all of them. A constant flow-rate of 50 l/h is used in both PVT collectors (Herrando et al., 2018a).

$$\eta_{th} = 0.472 - 9.5 \cdot T_r \quad \text{(eq. 1)}$$

$$T_r = \frac{(T_{fm} - T_a)}{I_t} \quad \text{(eq. 2)}$$

$$\eta_e = 0.1844 \cdot \left(1 - 0.0039 \cdot \left(T_{PV} - T_{ref}\right)\right) \quad \text{(eq. 3)}$$

where T_r is the reduced temperature, I_t (W/m^2) is the total global solar irradiance on the surface at a tilted angle, T_{fm} is the mean fluid temperature, T_a is the ambient temperature, T_{PV} is the PV cell temperature and T_{ref} is 25 °C (value given by the manufacturer).

Stratified water storage tanks

The tanks are modelled using a stratified water storage tank of constant fluid mass (Type 534), considering six fully mixed equal-volume segments that divide the cylinder along its vertical axis. In the hot-water tank, preheated water for heat at 60 °C demand is supplied via a port at the top of the tank, and water is refilled by mains water from the bottom node. One immersed heat exchanger connected to the PVT collector array runs from the middle (n=3) to the bottom of the tank (n=6), and another one connected with the a-w VC unit runs from the top (n=1) to the next node (n=2) to heat the water inside the tank to the set-point temperature (see Fig. 1 left). The stratified inertia tank that satisfies the low-temperature heating also has two immersed heat exchangers connected with the PVT collector array (from n=3 to n=6) and with the a-w VC unit (from n=1 to n=2), and a third immersed heat exchanger that heats the water for low-temperature heating, or cools the water for cooling, depending on the operation mode, in a closed-loop. The cooling demand is satisfied through this second storage tank, with the a-w VC unit working in cooling mode and the PVT collector array working at night. The storage tanks' volumes are varied through the variation of the V_t/A_{cT} ratio, where V_t is the tank volume (L) and A_{cT} is the total solar collector area (m^2). The size of the solar immersed heat exchanger coils also varies with the tank size through the variation of the tank height.

rev-VC unit

The reversible Vapour-Compression (VC) unit acts as an auxiliary heating/cooling. The unit is modelled using Type 941, and the data files (performance data) are modified to fit the real performance of the rev-VC unit (e.g. temperatures, COP, electricity consumption) provided by the manufacturer. Based on the thermal energy demands of the industrial building, the Yutaki S6 model (RWM-6.0) from Hitachi is selected (Hitachi), with a nominal thermal power of 16 kW for heating and 13.7 kW for cooling.

2.3 Key Performance Indicators

A set of Key Performance Indicators (KPIs) are defined to analyse the different solar configurations considered in this work, based on a report of Subtask D of Task 60 (IEA, 2018):

- Thermal energy yield per m^2 (Q_{PVT}, kWh/m^2): thermal energy output of the PVT collectors per m^2
- Electrical energy yield (E_{PVT}, kWh/m^2): electricity output of the PVT collectors per m^2
- Solar fractions: defined as the energy demand covered divided by the total energy demand: Solar thermal fraction of heat at 60ºC ($f_{s,H60}$), low-temperature heat ($f_{s,lth}$), radiative cooling ($f_{s,c-r}$), solar electrical fraction of cooling ($f_{s,c-e}$) and electricity demand ($f_{s,e}$).
- Investment cost (C_0, €/m^2): estimated from price lists available from solar retailers in the EU (Barilla Solar, 2017; Viridian Solar, 2017; Wagner Renewable, 2017). The cost of the storage tank is estimated using a correlation based on market prices of existing tanks across a range of storage volumes (Herrando et al., 2018b). The total installation costs are also considered. The main costs are associated with the vapour compression unit (42%) and the PVT collectors and support structures (27%).
- Payback time (*PBT*, years): defined as the period of time required to recover the investment cost (Herrando et al., 2018b; Kalogirou, 2014), is estimated:

$$PBT = \frac{ln\left[\frac{C_0 \cdot (i_F - d)}{AS} + 1\right]}{ln\left(\frac{1+i_F}{1+d}\right)} \quad \text{(eq. 4)}$$

where d is the discount rate (5%) (International Energy Agency (IEA), 2010; Kim et al., 2012) and i_F is the fuel inflation rate (3.5%) (Herrando et al., 2019a). The annual savings (*AS*) refer to the difference between the current annual costs that the industrial building incurs to cover all the energy demand (e.g. business as usual scenario, AC_{bau}), and the annual costs that the building would incur to cover all the energy demand if the proposed solar system was installed (AC_{ss}):

$$AS = AC_{bau} - AC_{ss} \quad \text{(eq. 5)}$$

$$AC_{bau} = E_{El,dem} \cdot c_e + \frac{Q_{H60,dem}}{COP} \cdot c_e + \frac{Q_{lth,dem}}{COP} \cdot c_e + \frac{Q_{Cool,dem}}{COP} \cdot c_e \quad \text{(eq. 6)}$$

$$AC_{ss} = E_{grid} \cdot c_e + E_{exc} \cdot s_e \quad \text{(eq. 7)}$$

where $E_{El,dem}$ refers to the electricity demand of the factory, $Q_{H60,dem}$ is the demand of heat at 60 °C, $Q_{lth,dem}$ is the low-temperature heat demand, $Q_{Cool,dem}$ is the cooling demand, E_{grid} is the electricity demand that cannot be covered by the proposed solar system and thus should be imported from the grid, E_{exc} is the electricity excess exported to the grid and imported later on via net metering, c_e is the electricity price (0.244 €/kWh) and s_e is electricity price for the net metering option (0.122 €/kWh).

3. Results and discussion

Initial validation was undertaken at the component level. For the PVT collectors, the electrical efficiency curve obtained in the simulation is within 2% of the respective efficiency provided by the manufacturer, while the thermal efficiency is within 5%, except for T_r > 0.045. However these high T_r values are for T_{in} > 70 °C; and uncovered PVT collectors are not usually operated at temperatures higher than 70 °C, because thermal losses at these temperatures are larger than thermal gains, and therefore water is cooled, rather than heated, in the collector. The performance of the rev-VC unit was validated with the manufacturers' data, integrated into the TRNSYS type.

3.1 Sensitivity Analysis

A series of sensitivity analyses were undertaken to optimise the system's performance and minimise the system's payback time. The modified parameters were the number of PVT collectors with the corresponding solar collector area (A_{cT}), and the sizes of the storage tanks, including the volume of the hot-water tank (V_{t1}) and the volume of the inertia tank (V_{t2}). Table 2 summarises the parameters' values as well as the main results for the different analysed cases.

The priority given for the electricity generated by the PVT collectors is to cover: 1) electricity consumed by the rev-VC for cooling ($E_{Cool.rVC}$), 2) electricity demand ($E_{El.dem}$), 3) electricity consumed by the rev-VC for low-temperature heat ($E_{lth,rVC}$), 4) electricity consumed by the rev-VC for heat at 60 °C ($E_{H60,rVC}$).

Tab. 2: Summary of analysed cases and annual energy results for the studied industrial building.

Variable	Analysed Cases					
	C1	C2	C3	C4	C5	C6
***Nº PVT collectors* (-)**	16	16	16	30	30	30
A_{cT} (m^2)	26.1	26.1	26.1	48.9	48.9	48.9
V_{t1} (L)	350	600	950	500	500	500
V_{t2} (L)	350	350	350	500	1000	1500
V_t=V_{t1}+V_{t2} (L)	700	950	1400	1000	1500	2000
V_{t1} /A_{cT} (L/m^2)	13.4	23.0	36.4	10.2	10.2	10.2
V_{t2} /A_{cT} (L/m^2)	13.4	13.4	13.4	10.2	20.4	30.7
V_t /A_{cT} (L/m^2)	26.8	36.4	49.8	20.5	30.7	40.9
$T_{max,t1}$ (°C)	71.7	70.1	64.8	72.4	72.4	72.4
$T_{max,t2}$ (°C)	41.8	41.7	41.7	41.5	40.8	40.7
Q_{PVT} (kWh/m^2)	101.6	104.9	117.5	69.2	71.6	72.8
E_{PVT} (kWh/m^2)	242.2	242.4	242.7	241.5	241.6	241.6
$f_{s,H60}$ (%)	60.4%	63.7%	60.9%	68.3%	68.1%	68.4%
$f_{s,lth}$ (%)	4.6%	4.4%	4.1%	7.5%	8.7%	9.3%
$f_{s,c-r}$ (%)	13.5%	13.5%	13.5%	19.2%	34.9%	46.5%
$f_{s,c-e}$ (%)	49.5%	49.6%	48.6%	94.5%	95.4%	94.8%
$f_{s,e}$ (%)	31.7%	31.7%	31.7%	48.2%	48.5%	48.5%
C_0 (€/m^2)	850	858	870	656	665	674
***PBT* (years)**	8.7	8.9	8.9	9.4	9.6	9.7

The results show that, for the same number of PVT collectors, increasing the hot-water tank volume (cases C1-C3) leads to larger thermal energy yield per m^2 (Q_{PVT}), which is attributed to the larger thermal storage capacity per m^2 (V_{t1} /A_{cT}). Similarly, increasing the inertia tank volume (C4-C6) also leads to larger thermal energy yield per m^2, for the same reason (larger V_{t2} /A_{cT} in this case). However, the thermal energy yield per m^2 is lower for the cases with more PVT collectors, because of the lower total thermal storage capacity m^2 (V_t /A_{cT}) and the consequently higher tank temperature, as shown in Table 2. The water that passes through the PVT collectors is hotter and thus the collectors work at a lower thermal efficiency.

The solar thermal fraction of heat at 60ºC ($f_{s,H60}$) is larger in cases C4 to C6 due to the higher temperature of the hot-water tank, and the larger number of PVT collectors (larger A_{cT}) and thermal storage capacity (V_t). Similarly, the solar thermal fraction of low-temperature heat ($f_{s,lth}$) and the solar thermal fraction of the radiative cooling ($f_{s,c-r}$) are larger as the inertia tank volume (V_{t2}) increases, as expected. It is observed that the latter ($f_{s,c-r}$) considerably increases with the size of this tank, increasing from 19.2% to 46.5% when the inertia tank volume (V_{t2}) is tripled.

The solar electrical fraction of cooling ($f_{s,c-e}$) considerably increases with the number of PVT collectors (cases C4 to C6), as more electricity is generated and thus a larger percentage of the electricity consumed by the rev-VC unit for cooling is covered, with values between 94.5% and 94.8%. The solar electricity fraction of electricity demand ($f_{s,e}$) also increases with the number of PVT collectors, but al less extent, from 31.7% to 48.5% (see cases C4 to C6). The reason attributed is the priorities set within the system, as first the electricity consumed by the rev-VC unit for cooling is covered, and then the excess is used to cover the electricity demand of the building (lighting and other devices).

The system's payback time is larger for the systems with 30 PVT collectors, despite the lower investment cost per m^2 (cases C4 to C6). The main reason attributed to this is the more profitable use of the electricity generated by the PVT collectors. As the number of PVT collectors increases, there is more excess electricity, that is, a larger fraction of the electricity generated cannot be instantaneously used to cover the demand, and thus it has to be exported to the grid, and imported later on when there is more demand than generation. However, the price at

which the electricity exported and imported later on is lower than the electricity price (half in this case, as shown in Section 2.3), so larger economic savings are achieved when the electricity is directly used in the building.

Based on these results, the component dimensions of case C1 are selected to build the pilot plant: 16 PVT collectors, with a total solar PVT area of 26.1 m^2; tank volumes, V_{t1} and V_{t2}, of 350 L each one, which implies a total accumulation volume of 700 L, and a ratio V_t/A_{cT} of 26.8. The following section shows the transient results obtained for this case (C1).

3.2 Transient Results of the selected S-CCHP system

This section presents the results of the selected configuration during nine consecutive days in summer (when there is cooling demand) and in winter (when there is low-temperature heat demand).

Figure 2 shows that at night (when there is no solar irradiance, yellow continuous line), the water temperature at the outlet of the PVT collectors drops (dark-red dashed-dotted line). When it is below the water temperature at the bottom of the inertia tank (orange dotted line), the water enters the immersed heat exchanger to cool down the inertia tank. Thanks to this, it is observed that a part of the cooling demand (dashed purple line) can be covered with the radiative cooling (violet continuous line).

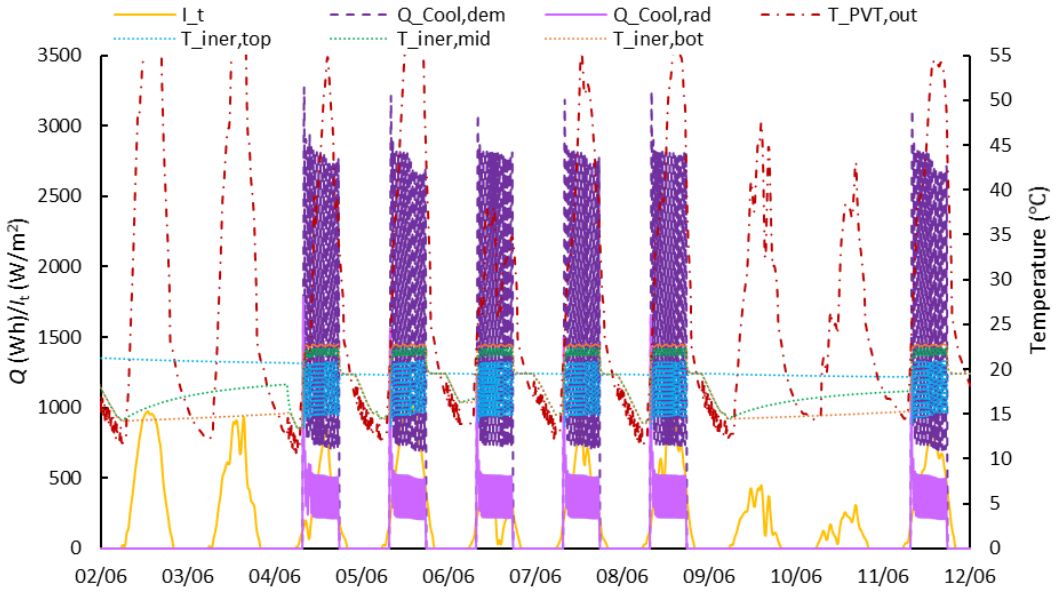

Fig. 2: Total solar irradiance at tilted angle (I_t), cooling demand ($Q_{Cool,dem}$), cooling demand covered with radiative cooling ($Q_{Cool,rad}$), PVT water output temperature ($T_{PVT,out}$), water temperature at the top of the inertia tank ($T_{iner,top}$), water temperature at the middle of the inertia tank ($T_{iner,mid}$), and water temperature at the bottom of the inertia tank ($T_{iner,bot}$) during 2-11 June.

The cooling demand not covered with the radiative cooling is satisfied by the rev-VC unit, which cools down the inertia tank to the required temperature. The electricity consumed by this unit is shown in Figure 3 (dark-blue dotted line, $E_{Cool.rVC}$), as well as the electricity instantaneously covered (light-blue continuous line, $E_{Cool.cov}$) with the PVT electrical output (red continuous line). It is observed that on sunny days, a considerable amount of the energy consumed by the rev-VC for cooling is instantaneously covered, as it occurs during the days when solar irradiance is high (yellow continuous line). The rest of the electricity is used to cover the electricity demand of the industry (dashed purple line). It is observed that during the first weekend (first two days of Figure 3) when there is no cooling demand, all the electricity demand of the industry is covered (violet continuous line). Instead, due to the low irradiance levels during the second weekend (yellow continuous line), the electricity demand is only partially covered.

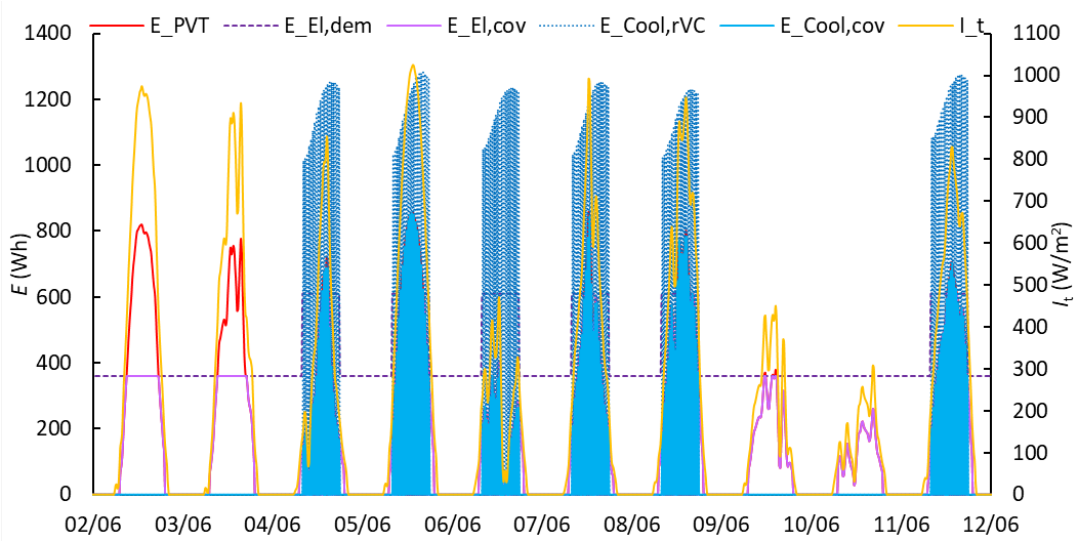

Fig. 3: Total electricity generated (E_{PVT}), electricity demand ($E_{El,dem}$), electricity demand instantaneously covered ($E_{El,cov}$), electricity consumed by the rev-VC for cooling ($E_{Cool,rVC}$), electricity consumed by the rev-VC for cooling instantaneously covered ($E_{Cool,cov}$), and total solar irradiance at tilted angle (I_t) during 2-11 June.

Figure 4 shows the low-temperature heat demand (dashed purple line, $Q_{lth,dem}$), along with the part covered by the PVT thermal output (violet continuous line, $Q_{lth,cov}$). The system gives priority to heat the water in the inertia tank until 40 °C, thus, during the first weekend, when there are not heating demands, water from the PVT collectors heats the inertia tank until it reaches 40 °C (see dark-red and green dotted lines). Afterwards, early in the morning, part of the low-temperature heat demand is covered with the PVT thermal output. The rest of the demand is covered by the rev-VC unit (see Figure 6), which heats the water at the top of the tank (dark-red dotted line).

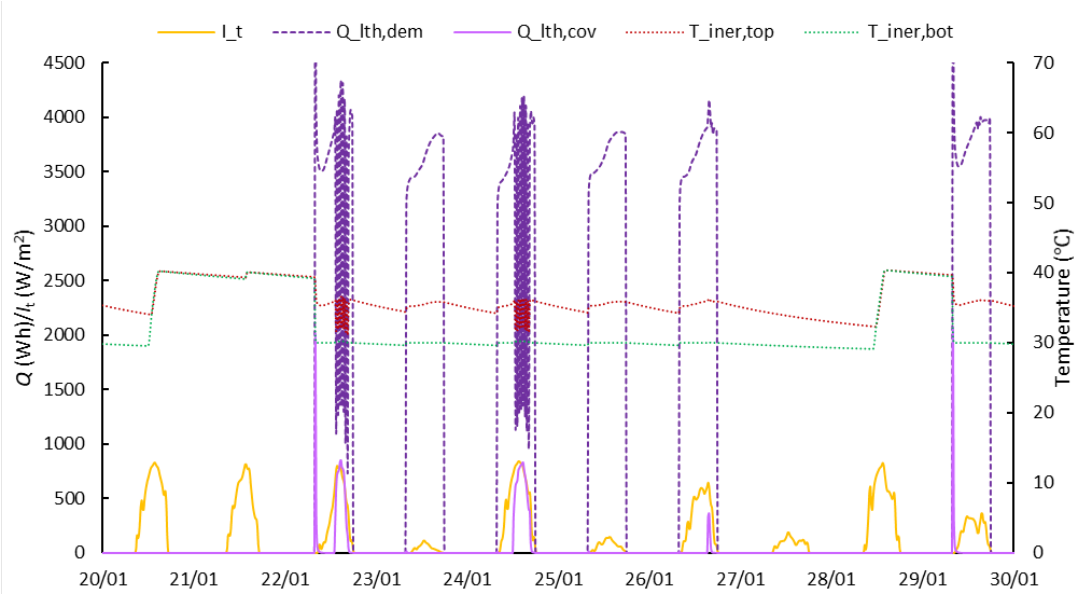

Fig. 4: Total solar irradiance at tilted angle (I_t), low-temperature heat demand ($Q_{lth,dem}$), low-temperature heat demand covered ($Q_{lth,cov}$), water temperature at the top of the inertia tank ($T_{iner,top}$) and water temperature at the bottom of the inertia tank ($T_{iner,bot}$) during 20-29 January.

As shown in Figure 5, the demand for heat at 60 °C (dark-blue dotted line, $Q_{H60,dem}$) is constant from Monday to Friday at working hours. The PVT thermal output heats the water in the hot-water tank after the inertia tank reaches 40 °C, increasing the water temperature (red dashed-dotted line), so part of the demand of heat at 60 °C is covered (light-blue continuous line). The rest of the demand is covered by the rev-VC unit, which heats the

water at the top of the tank until it reaches the set-point (red dashed-dotted line).

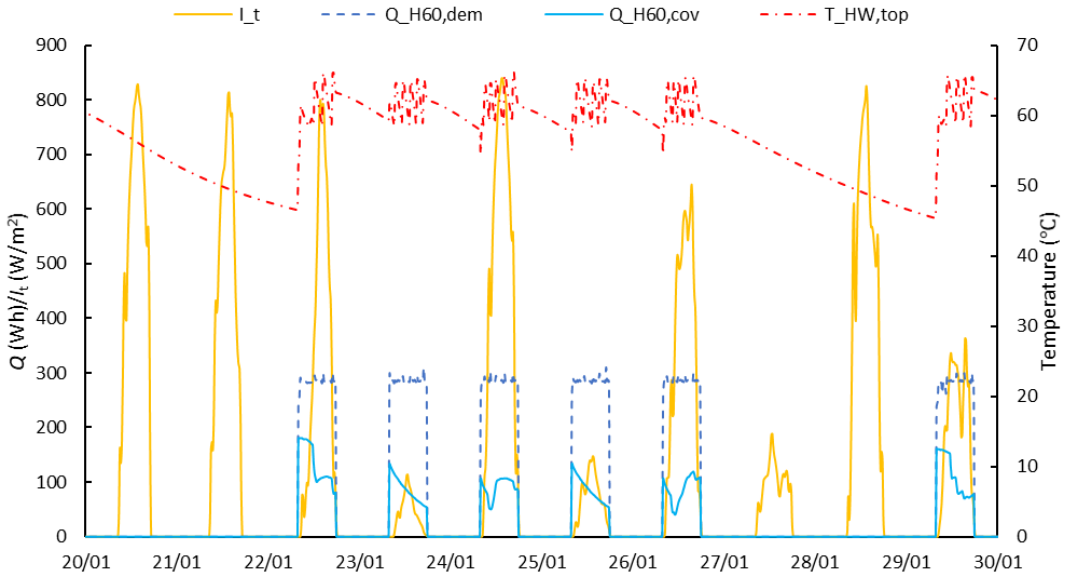

Fig. 5: Total solar irradiance at tilted angle (I_t), demand of heat at 60 °C ($Q_{H60,dem}$), demand of heat at 60 °C covered ($Q_{H60,cov}$low-temperature heat demand covered ($Q_{lth,cov}$), and water temperature at the top of the hot-water tank ($T_{HW,top}$), during 20-29 January.

The heating demands not covered with the PVT thermal output are satisfied by the rev-VC unit, which heats the tanks to the required temperatures. The electricity consumed by this unit for low-temperature heat (dark-blue dotted line, $E_{lth,rVC}$) is shown in Figure 6 and for heat at 60 °C (dashed purple line, $E_{H60,rVC}$) is shown in Figure 7. Figure 6 shows that during the week, the days with a large PVT electrical output (red continuous line), due to high irradiance levels (yellow continuous line), that is, 22nd and 24th of January, part of the low-temperature heat demand is instantaneously covered by the PVT electrical output (light-blue continuous line, $E_{lth,cov}$). However, the rest of the days, with a lower electricity generation, only a limited amount of the low-temperature heat demand is instantaneously covered.

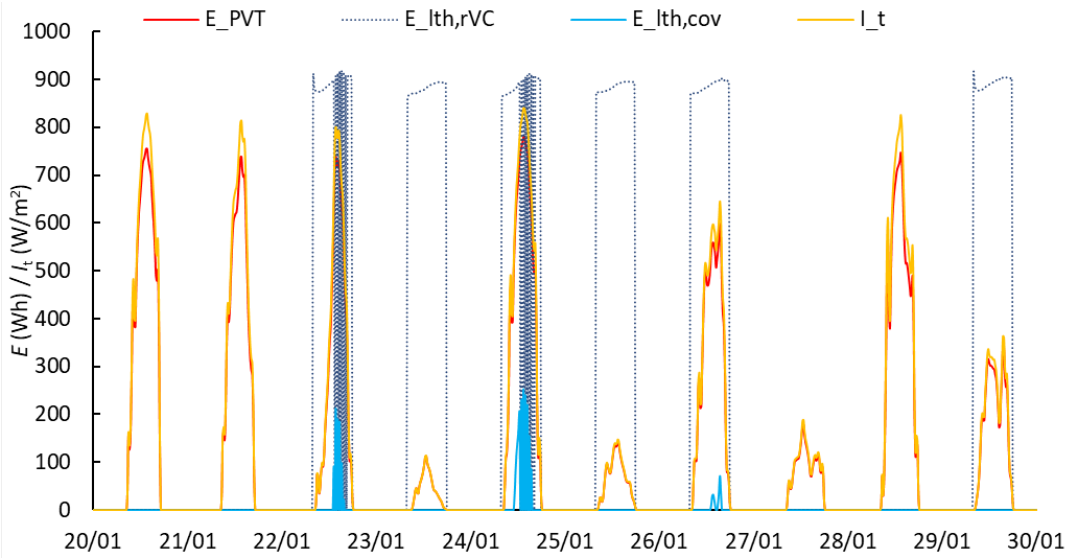

Fig. 6: Total electricity generated (E_{PVT}), electricity consumed by the rev-VC for low-temperature heat ($E_{lth,rVC}$), electricity consumed by the rev-VC for low-temperature heat instantaneously covered ($E_{lth,cov}$), and total solar irradiance at tilted angle during 20-29 January.

Figure 7 shows that only a very limited amount of the electricity consumed by the rev-VC unit for heat at 60 ºC (dashed purple line, $E_{H60,rVC}$) is instantaneously covered by the PVT electrical output, negligible during the days shown here (violet continuous line, $E_{H60,cov}$). This is attributed to the priorities given within the system, as the electricity consumed by the rev-VC for heat at 60 ºC is the last one to be satisfied, as explained in Section 3.1.

It is observed that during the first weekend there is a considerable excess of electricity (dashed-dotted green line) which is fed into the grid, to be imported later on to cover the electricity consumed during the night. The reason is the large PVT electrical output (red continuous line) due to the high irradiance levels (yellow continuous line), along with the fact that during the weekend there are no heating and cooling demands. Conversely, the low irradiance levels of the first day of the second weekend (27th Jan) lead to low electricity generation and thus there is no electricity surplus.

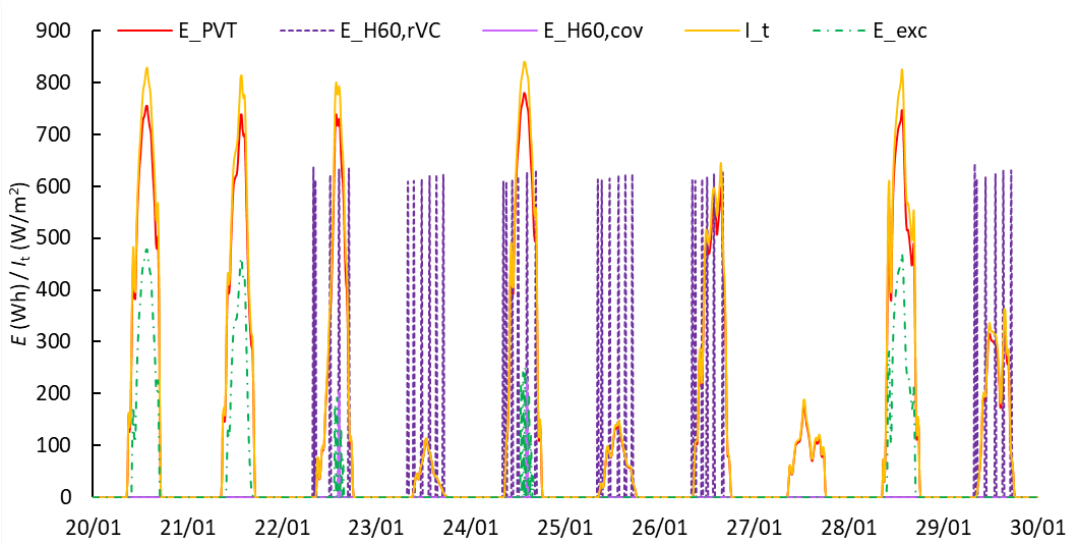

Fig. 7: Total electricity generated (E_{PVT}), electricity consumed by the rev-VC for heat at 60 ºC ($E_{H60,rVC}$), electricity consumed by the rev-VC for heat at 60 ºC instantaneously covered ($E_{H60.cov}$), electricity surplus fed into the grid (E_{exc}) and total solar irradiance at tilted angle during 20-29 January.

4. Conclusions

This paper presents the techno-economic performance of several S-CCHP system configurations that feature PVT collectors, thermal storage and an air-to-water (a-w) reversible vapour-compression (rev-VC) unit, for cooling, heating and power provision to an industrial building. The real heating, cooling and electricity demands of an industrial building located in Zaragoza (Spain) are used as inputs to the transient model developed.

In the proposed systems, the PVT thermal output is used to heat the water of two parallel storage tanks, one that provides heat at 60ºC (hot-water tank) and another one that satisfies low-temperature heat in winter and cooling in summer (inertia tank). In summer, water circulates at night through the PVT collectors to cool the water in the inertia tank (radiative cooling). The PVT electrical output is to used cover the electricity demand as well as the electricity consumed by the rev-VC to provide the rest of the cooling, low-temperature heat and heat at 60 ºC demands.

The results show that the S-CCHP systems have the potential to cover 19.2% to 46.5% of the cooling demand with radiative cooling, depending on the number of PVT collectors, decreasing the electricity consumed by the rev-VC unit. Of the latter, ~50% and ~95% can be covered with the PVT electrical output, with 16 and 30 PVT collectors respectively. All the analysed configurations can also cover >60% of the demand for heat at 60ºC and between 31.7% to 48.5% of the electricity demand (lighting and other devices) of the analysed building.

The economic analysis shows that the lower price at which the electricity exported is imported later on compared to the electricity price (half in this case) influences the profitability of the system. As a consequence, lower economic savings are achieved as the electricity directly used in the building decreases, that is, as the electricity excess increases. Still, all the proposed configurations have a payback time of <10 years. The selected S-CCHP

system configuration, 16 PVT collectors (26.1 m^2) and 2 tanks of 350 L each one, is currently being manufactured and will be tested under real weather conditions from middle September 2020.

5. Acknowledgements

This work was undertaken in the framework of 3GSol project, funded under the Retos-Colaboración 2017 Programme, National R&D and Innovation Plan, by the Spanish Government, Ministry of Science, Innovation and Universities and cofunded by the EU, through the European Regional Development Fund (ERDF) [grant number RTC-2017-6026-3].

6. References

Barilla Solar, 2017. Wholesale Solar Thermal Supplies Barilla Solar http://www.barillasolar.co.uk/ (accessed 7.19.17).

Bellos, E., Tzivanidis, C., Moschos, K., Antonopoulos, K.A., 2016. Energetic and financial evaluation of solar assisted heat pump space heating systems. Energy Convers. Manag. 120, 306–319. https://doi.org/10.1016/J.ENCONMAN.2016.05.004

Das, D., Kalita, P., Roy, O., 2018. Flat plate hybrid photovoltaic- thermal (PV/T) system: A review on design and development. Renew. Sustain. Energy Rev. 84, 111–130. https://doi.org/10.1016/j.rser.2018.01.002

EndeF, 2017. Endef - Energy, Development and Future. http://endef.com (accessed 2.10.17).

European Commission, 2016. An EU strategy on heating and cooling. Communication from the Commission to the European Parliament, the Council, the European Economic and Social Committee and the Committee of the Regions.

European Union, 2018. Energy in figures – Statistical pocketbook.

Ge, T.S., Wang, R.Z., Xu, Z.Y., Pan, Q.W., Du, S., Chen, X.M., Ma, T., Wu, X.N., Sun, X.L., Chen, J.F., 2018. Solar heating and cooling: Present and future development. Renew. Energy 126, 1126–1140. https://doi.org/10.1016/J.RENENE.2017.06.081

Herrando, M., Pantaleo, A.M., Wang, K., Markides, C.N., 2019a. Solar combined cooling, heating and power systems based on hybrid PVT, PV or solar-thermal collectors for building applications. Renew. Energy 143, 637–647. https://doi.org/10.1016/j.renene.2019.05.004

Herrando, M., Ramos, A., Freeman, J., Zabalza, I., Markides, C.N., 2018a. Technoeconomic modelling and optimisation of solar combined heat and power systems based on flat-box PVT collectors for domestic applications. Energy Convers. Manag. 175, 67–85. https://doi.org/10.1016/j.enconman.2018.07.045

Herrando, M., Ramos, A., Zabalza, I., 2018b. Cost competitiveness of a novel PVT-based solar combined heating and power system: Influence of economic parameters and financial incentives. Energy Convers. Manag. 166, 758–770. https://doi.org/10.1016/j.enconman.2018.04.005

Herrando, M., Ramos, A., Zabalza, I., Markides, C.N., 2019b. A comprehensive assessment of alternative absorber-exchanger designs for hybrid PVT-water collectors. Appl. Energy 235, 1583–1602. https://doi.org/10.1016/J.APENERGY.2018.11.024

Hitachi, YUTAKI S COMBI. https://www.hitachiaircon.es/gamas/aerotermia/yutaki-s-combi (accessed 20.8.20).

IEA, 2018. Task 60: PVT Systems: Application of PVT Collectors and New Solutions in HVAC Systems, Solar Heating and Cooling Programme.

International Energy Agency (IEA), 2010. Projected Costs of Generating Electricity.

Joshi, S.S., Dhoble, A.S., 2018. Photovoltaic -Thermal systems (PVT): Technology review and future trends. Renew. Sustain. Energy Rev. 92, 848–882. https://doi.org/10.1016/j.rser.2018.04.067

Kalogirou, S.A., 2014. Solar energy engineering: processes and systems, Second Edi. ed. Academic Press. https://doi.org/10.1016/B978-0-12-374501-9.00014-5

Kim, Y., Thu, K., Kaur, H., Singh, C., Choon, K., 2012. Thermal analysis and performance optimization of a solar hot water plant with economic evaluation. Sol. Energy 86, 1378–1395. https://doi.org/10.1016/j.solener.2012.01.030

Klein, S.A., 2016. TRNSYS 18: A Transient System Simulation Program.

Leonzio, G., 2017. Solar systems integrated with absorption heat pumps and thermal energy storages: state of art. Renew. Sustain. Energy Rev. 70, 492–505. https://doi.org/10.1016/J.RSER.2016.11.117

Montagnino, F.M., 2017. Solar cooling technologies. Design, application and performance of existing projects. Sol. Energy 154, 144–157. https://doi.org/10.1016/J.SOLENER.2017.01.033

Thygesen, R., Karlsson, B., 2014. Simulation and analysis of a solar assisted heat pump system with two different storage types for high levels of PV electricity self-consumption. Sol. Energy 103, 19–27. https://doi.org/10.1016/j.solener.2014.02.013

Vaishak, S., Bhale, P. V., 2019. Photovoltaic/thermal-solar assisted heat pump system: Current status and future prospects. Sol. Energy 189, 268–284. https://doi.org/10.1016/j.solener.2019.07.051

Viridian Solar, 2017. The Pod - Solar Water Heating Simplified. http://www.viridiansolar.co.uk/solar-products-solar-heating-with-combi-pod.html (accessed 7.19.17).

Wagner Renewable, 2017. Home Page - Wagner Renewables Ltd. http://www.wagnersolarshop.com/ (accessed 7.19.17).